

Model-independent constraints on exotic particle masses from lepton decays and the role of interference

Mario W. Barela*

*Instituto de Física Teórica, Universidade Estadual Paulista,
R. Dr. Bento Teobaldo Ferraz 271, Barra Funda
São Paulo - SP, 01140-070, Brazil.*

J. Montaña-Domínguez†

*Conacyt-Facultad de Ciencias Físico Matemáticas,
Universidad Michoacana de San Nicolás de Hidalgo,
Av. Francisco J. Múgica s/n, 58060, Morelia, Michoacán, México.*

Together with every Beyond the Standard Model ultraviolet complete, renormalizable model, several exotic particles are usually hypothesized. CP -even neutral and doubly-charged scalars are common, well-known examples which can contribute to the seven 3-body Charged Lepton Flavor Violating decays. The experimental bounds on each Branching Ratio within this set of processes provide a good test for new physics that can induce powerful constraints on relevant parameter spaces. This is specially true for a third species of particle which, unlike the previous two, is a rare feature of renormalizable models: a doubly charged vector bilepton. We show how these purely leptonic bounds can indeed induce relevant exclusion regions for the corresponding particles masses, stronger than what have been considered in the literature, and examine how interference effects can influence these regions in a non-trivial way.

I. INTRODUCTION

Despite its phenomenal success in justifying and describing some of the most complex experimental results, including high precision data and the confirmed Higgs boson prediction, the Standard Model (SM) of elementary particles and fundamental interactions presents several problems. These include the inability of accounting for urgent theoretical physical issues, such as Neutrino Masses, Dark Matter or Matter-Antimatter Asymmetry, and other aspects which may be interpreted as matters of elegance or non-optimal construction, like the Hierarchy Problem or the arbitrariness in the number of families. From this, emerged the necessity of Beyond the Standard Model (BSM) physics, whose classes of most elegant tentative instances are Grand Unified Theories (GUT) and Supersymmetry. Once these types of theories have, at least, not been encouraged at the LHC scales, models with, in principle, lower characteristic scales, conceptually similar to the SM, with a non-simple Gauge Group, have began to be examined.

Independently of the species of extension or alternative model, the new constructions generally imply the introduction of new degrees of freedom, usually not immediately desirable by themselves. Among the examples of new physics generated together with exotic particles, is Charged Lepton Flavor Violation (CLFV). CLFV signatures are forbidden at tree level in the context of the SM, and hence are extremely useful in the quest of testing alternative hypotheses. Specifically, they can occur, in the SM, at the one-loop level and are, naturally, extremely suppressed: it is predicted that the main muon and tau branching ratios, $\mu \rightarrow 3e$, $\tau \rightarrow 3e$ and $\tau \rightarrow 3\mu$, for example, happen with order of magnitude $< 10^{-50}$ [1–4]. To date, there is no concrete direct sign of CLFV, and the status of this type of search is of improving sensitivity [5–11].

Besides being efficient because of virtually nonexistent SM background, CLFV is also a great prospect for BSM searches because it may be contained in most kinds of new physics models, such as Supersymmetry [12–15], 2HDM [16–18] and 3-3-1 models [19–22].

An interesting specific set of CLFV channels is that of the already mentioned 3-body lepton decays, *i.e.*, the decays of muons and taus into respective combinations of 3 lighter leptons. These processes enjoy the operational benefits of being purely leptonic: they are free of a number of complications present at LHC processes, specially hadron physics, which poses both computational *and* theoretical difficulties. For instance, it is hard to effect truly general and model-independent analysis on a number of BSM LHC processes because of highly model-dependent hadronization structures.

* mario.barela@unesp.br

† jmontano@conacyt.mx

The objective of this work is to investigate whether the simultaneous application of the bounds on the Branching Ratios (BR) of 3-body lepton decays is enough to achieve model-independent useful results regarding the masses of three species of exotic particles: an exotic flavor violating neutral scalar s , a doubly-charged scalar bilepton $Y^{\pm\pm}$ and a doubly-charged vector bilepton $U^{\pm\pm}$. Most important in our discussion is the vector bilepton, a rare particle present most notably in 3-3-1 models [23–25] and $SU(15)$ GUT [26, 27], which entails unitary mixing. Nevertheless, special attention will be paid on the occurring interferences when two distinct bosons are mediating the decays, to observe that such effects can impact in a meaningful way bounds on new BSM degrees of freedom.

The paper is organized as follows. In Section II relevant discussions concerning the model-independent parametrization of the relevant interactions are carried, and the corresponding effective Lagrangians presented. In Sec. III the charged LFV decay amplitudes contributing to a generic $\ell_i^+(p) \rightarrow \ell_i^+(k_1)\ell_j^+(k_2)\ell_k^-(k_3)$ are shown. The Sec. IV is devoted to show the results and discussing its consequences. Finally, our conclusions are addressed in Sec. V. In the Appendix A the non-trivial attainment of the amplitudes from Lagrangians that contain explicit charge conjugation is described, as well the corresponding Feynman rules presented. In the Appendix B, some numerical solutions are explicitly written.

II. OBJECTIVES AND EFFECTIVE INTERACTIONS

This work's main goal is to draw model-independent exclusion contours on the masses of 3 species of exotic particles, constraining theory space by taking advantage of the simultaneous data of 3-body lepton decay. The examined particles are the ones which can contribute to the relevant processes: doubly-charged vector bileptons $U^{\pm\pm}$; doubly-charged scalars $Y^{\pm\pm}$; and flavor violation mediating neutral scalars s .

In order to take into account and gain insight on interesting interference effects [28] and because it can be expected that there is more than just one exotic particle not contemplated by the SM, we consider two particles at a time.

Besides the aforementioned particles, a neutral vector boson Z' could also contribute to the relevant processes. This, however, can only happen in non-democratic underlying models, where distinct lepton families constitute different representations of the gauge group, otherwise the a priori diagonal kinetic terms result in a mixing matrix of the form $\mathcal{O}_{Z'} = V_L^\dagger V_L = \mathbb{1}$. Because of this, since we avoid focusing on specific models and, furthermore, non-democratic leptonic sectors being rare, we overlook the possible role of an exotic neutral vector boson.

A substantial aspect of the challenge resumes itself to a correct parametrization of the effective exotic interactions. Consider first the doubly-charged vector bilepton $U^{\pm\pm}$. The possible electric charge and handedness structure of the spinor chain limits the form of the most general $U\ell\ell$ interaction Lagrangian to be

$$\mathcal{L}_{U\ell\ell} = \sum_a g_U \overline{\ell'_a{}^c} \gamma^\mu \ell'_{aL} U_\mu^{++} + g_U \overline{\ell'_{aL}} \gamma^\mu \ell'_a{}^c U_\mu^{--}, \quad (1)$$

which is diagonal on lepton symmetry eigenstates, the primed fields, because it comes from a minimally coupled kinetic term and we only consider lepton universal models, as discussed above, and where the second term is merely the hermitian conjugate of the first one. Notice that unlike interactions which conserve fermion number, any single term in the sum exhausts the degrees of freedom of a single fermion. Hence, we may consider only the Lagrangian above, without writing a hand-mirrored term $g'_U \overline{\ell'_a{}^c} \gamma^\mu \ell'_{aR} U_\mu^{++}$ that would involve the same fields. In fact, $g'_U \overline{\ell'_a{}^c} \gamma^\mu \ell'_{aR} U_\mu^{++} = -g'_U \overline{\ell'_a{}^c} \gamma^\mu \ell'_{aL} U_\mu^{++}$, so that adding the second term would amount to a mere redefinition of the coupling.

The fermions are rotated to their mass eigenstates through the bi-unitary transformation $\ell'_{L(R)} \equiv V_{L(R)} \ell_{L(R)}$, from which follows (taking left-handed fields as the example)

$$\begin{aligned} \overline{\ell'_L} &= \overline{\ell_L} V_L^\dagger, \\ (\ell'^c)_L &= V_R^* (\ell^c)_L, \\ \overline{(\ell'^c)_L} &= \overline{(\ell^c)_L} V_R^T. \end{aligned} \quad (2)$$

With this we have, for mass eigenstates

$$\mathcal{L}_{U\ell\ell} = \sum_{a,b} g_U \overline{\ell'_a{}^c} \gamma^\mu P_L (V_U)_{ab} \ell_b U_\mu^{++} + g_U \overline{\ell'_a} \gamma^\mu P_L (V_U^\dagger)_{ab} \ell_b^c U_\mu^{--}, \quad (3)$$

where $V_U \equiv V_R^T V_L$ is a unitary matrix. However, because both fermions in any term above carry the same conserved charge, there are two terms that contribute to any vertex. We may transpose one of them to, after carrying the spinor

and charge conjugation algebra, rewrite the Lagrangian as

$$\begin{aligned} \mathcal{L}_{U\ell\ell} = & \sum_{b>a} g_U \left\{ \bar{\ell}_a^c \gamma^\mu [P_L(V_U)_{ab} - P_R(V_U)_{ba}] \ell_b U_\mu^{++} + \bar{\ell}_a \gamma^\mu [P_L(V_U^\dagger)_{ab} - P_R(V_U^\dagger)_{ba}] \ell_b^c U_\mu^{--} \right\} \\ & + \sum_a g_U \left\{ \bar{\ell}_a^c \gamma^\mu [P_L(V_U)_{aa}] \ell_a U_\mu^{++} + \bar{\ell}_a \gamma^\mu [P_L(V_U^\dagger)_{aa}] \ell_a^c U_\mu^{--} \right\}, \end{aligned} \quad (4)$$

with $a, b = e, \mu, \tau$. Notice that we have chosen to leave the heaviest lepton on the right. This exact manipulation and the resulting vertices are a common source of confusion.

Although g_U is, in general, a free parameter, if (i) the symmetry breaking pattern of the underlying model is such that $SU(2)_L \subset G$, where G is a simple group, and (ii) $U^{\pm\pm}$ is a maximally mixed combination of N of its gauge bosons, then $g_U = \frac{g_{2L}}{\sqrt{N}}$, where g_{2L} is the Standard Model $SU(2)_L$ gauge coupling. This follows from a matching condition at the breaking scale which dictates $g_G = g_{2L}$ [29]. Although this construction may seem to be a strong imposition, the charged vector bosons of many common models tend to satisfy these requirements as the theories generalize the standard model electric charge scheme in such a way that the adjoint charge eigenstates are usually proportional $\frac{T_i \pm iT_j}{\sqrt{2}}$, where $T_{i,j}$ are two generators of the gauge algebra. We use this to completely fix g_U numerically, selecting the case where $U^{\pm\pm}$ is a combination of 2 gauge bosons, and write $g_U = \frac{g_{2L}}{\sqrt{2}}$. This construction corresponds, for instance, precisely to the case of the 3-3-1 model, but should cover a considerable sector of theory space. We write the final $U\ell\ell$ effective Lagrangian

$$\begin{aligned} \mathcal{L}_{U\ell\ell} = & \sum_{b>a} \frac{g_{2L}}{\sqrt{2}} \left\{ \bar{\ell}_a^c \gamma^\mu [P_L(V_U)_{ab} - P_R(V_U)_{ba}] \ell_b U_\mu^{++} + \bar{\ell}_a \gamma^\mu [P_L(V_U^\dagger)_{ab} - P_R(V_U^\dagger)_{ba}] \ell_b^c U_\mu^{--} \right\} \\ & + \sum_a \frac{g_{2L}}{\sqrt{2}} \left\{ \bar{\ell}_a^c \gamma^\mu [P_L(V_U)_{aa}] \ell_a U_\mu^{++} + \bar{\ell}_a \gamma^\mu [P_L(V_U^\dagger)_{aa}] \ell_a^c U_\mu^{--} \right\}. \end{aligned} \quad (5)$$

From which the interaction between same flavor leptons may be perceived to be purely axial: $\bar{\ell}_a^c \gamma^\mu P_L \ell_a = -\bar{\ell}_a^c \gamma^\mu \frac{\gamma^5}{2} \ell_a$.

Now we turn to the doubly-charged scalar. While the previous interaction was originated by the higher symmetry covariant derivative, this one comes from Yukawa Lagrangians. We have as the most general effective interactions

$$\mathcal{L}_{Y\ell\ell} = - \sum_{a,b} g_{YL} \left\{ \bar{\ell}_a^c (\mathcal{O}_Y)_{ab} P_L \ell_b Y^{++} + \bar{\ell}_a (\mathcal{O}_Y^\dagger)_{ab} P_R \ell_b^c Y^{--} \right\}. \quad (6)$$

In the Lagrangian above, the fermions are already mass eigenstates and the interaction mixing matrix is arbitrary: it is related to one a priori (arbitrary) Yukawa matrix G_Y as $\mathcal{O}_Y = V_R^T G_Y V_L$. By the reasoning above, it is not necessary to add a second handedness term.

We can once more work with both terms in Eq. (6) that involve a pair a, b of (equal charge) leptons in order to arrange them into an identical spinor chain, after which we obtain the final Lagrangian for this interaction:

$$\begin{aligned} \mathcal{L}_{Y\ell\ell} = & - \sum_{b>a} g_{YL} \left\{ \bar{\ell}_a^c [(\mathcal{O}_Y)_{ab} + (\mathcal{O}_Y)_{ba}] P_L \ell_b Y^{++} + \bar{\ell}_a [(\mathcal{O}_Y^\dagger)_{ab} + (\mathcal{O}_Y^\dagger)_{ba}] P_R \ell_b^c Y^{--} \right\} \\ & - \sum_{a=b} g_{YL} \left\{ \bar{\ell}_a^c [(\mathcal{O}_Y)_{aa}] P_L \ell_a Y^{++} + \bar{\ell}_a [(\mathcal{O}_Y^\dagger)_{aa}] P_R \ell_a^c Y^{--} \right\}. \end{aligned} \quad (7)$$

Lastly, we write the neutral scalar interaction Lagrangian. Lorentz and electric charge invariance dictates it must be simply

$$\begin{aligned} \mathcal{L}_{s\ell\ell} = & -g_{sL} \bar{\ell} \mathcal{O}_s P_L \ell s - g_{sL} \bar{\ell} \mathcal{O}_s^\dagger P_R \ell s \\ = & - \sum_{a,b} g_{sL} \bar{\ell}_a [(\mathcal{O}_s)_{ab} P_L + (\mathcal{O}_s^\dagger)_{ab} P_R] \ell_b s, \end{aligned} \quad (8)$$

where \mathcal{O}_s is arbitrary and related to a Yukawa matrix as $\mathcal{O}_s = V_R^\dagger G_s V_L$.

Obviously, the appropriate effective model also contains kinetic terms defined by

$$\begin{aligned} \mathcal{L}_{\text{kin}} = & -\frac{1}{2} U_{\mu\nu}^\dagger U^{\mu\nu} + M_U^2 (U^{++})^\dagger U^{++} \\ & + (\partial_\mu Y^{++})^\dagger \partial^\mu Y^{++} - M_Y^2 (Y^{++})^\dagger Y^{++} \\ & + \frac{1}{2} \partial_\mu s \partial^\mu s - \frac{1}{2} M_s^2 s^2, \end{aligned} \quad (9)$$

TABLE I: Number of parametric degrees of freedom contained within each scenario if the mixing matrices are regarded as complex and real.

Scenario	Complex	Real
$U - Y$	23	11
$U - s$	29	14
$s - Y$	32	17

where $U_{\mu\nu} = \partial_\mu U_\nu^{++} - \partial_\nu U_\mu^{++}$.

Three 2-particle scenarios will be considered, each with a pair of exotic species which interfere. The correspondent Lagrangians are

$$\begin{aligned}\mathcal{L}_{U-s} &= \mathcal{L}_{\text{kin}} + \mathcal{L}_{U\ell\ell} + \mathcal{L}_{s\ell\ell}, \\ \mathcal{L}_{U-Y} &= \mathcal{L}_{\text{kin}} + \mathcal{L}_{U\ell\ell} + \mathcal{L}_{Y\ell\ell}, \\ \mathcal{L}_{Y-s} &= \mathcal{L}_{\text{kin}} + \mathcal{L}_{Y\ell\ell} + \mathcal{L}_{s\ell\ell}.\end{aligned}\tag{10}$$

With a general, model-independent parametrization of the needed interactions, we may return to the central objective regarding which a few comments are in order. It is true that if the matrix elements of the 3 mixing matrices parametrizing the interaction Lagrangians could be arbitrarily small, any experimental constraint could be easily met; however, if these particles do exist *(i)* elements too small are not desirable because of matters such as naturalness and; *(ii)* more importantly, the theoretically predicted unitarity of the V_U matrix is powerful with respect to inducing exclusion contours.

Concerning the parameter space, notice that g_s and g_Y could be absorbed into their corresponding mixing matrices, and although we write them explicitly on analytical expressions (mostly for book keeping purposes) they will be effectively set to 1 in all numerical evaluations. Notice also, checking Eq. (7), that any matrix element of \mathcal{O}_Y only appears together with its symmetric partner, so that this effective mixing matrix may be taken symmetric. The free parameters in each scenario, which include masses and degrees of freedom of each matrix, may then be checked to be as appears on Table I.

Since to effect numerical optimization with the number of free parameters that exists when considering the general case is impractical, we considerably reduce the number of parameters by restricting the analysis to real matrices. The V_U unitary matrix then becomes an orthogonal one, whose determinant may be chosen to be 1 without loss of generality, and which we parametrize with Euler Angles

$$V_U = \begin{pmatrix} \cos\psi \cos\phi - \cos\theta \sin\phi \sin\psi & \cos\psi \sin\phi + \cos\theta \cos\phi \sin\psi & \sin\theta \sin\psi \\ -\sin\psi \cos\phi - \cos\theta \sin\phi \cos\psi & -\sin\psi \sin\phi + \cos\theta \cos\phi \cos\psi & \sin\theta \cos\psi \\ \sin\theta \sin\phi & -\sin\theta \cos\phi & \cos\theta \end{pmatrix}.\tag{11}$$

III. CALCULATIONS

The diagrams contributing to a generic $\ell_l^+(p) \rightarrow \ell_i^+(k_1)\ell_j^+(k_2)\ell_k^-(k_3)$ decay appear on Figure 1. The corresponding amplitudes are given by

$$\begin{aligned}i\mathcal{M}_U &= \left(\frac{ig_{2L}}{\sqrt{2}}\right)^2 \bar{v}_{\ell_l}(p)\gamma^\mu(V_{Ukl}P_L - V_{Ulk}P_R)v_{\ell_k}(k_3) \frac{-ig_{\mu\nu}}{(k_1+k_2)^2 - M_U^2} \\ &\quad \times \bar{u}_{\ell_i}(k_1)\gamma^\nu(V_{Uij}P_L - V_{Uji}P_R)v_{\ell_j}(k_2),\end{aligned}\tag{12}$$

$$\begin{aligned}i\mathcal{M}_Y &= (-ig_Y)^2 \bar{v}_{\ell_l}(p)(\mathcal{O}_{Ylk} + \mathcal{O}_{Ykl})P_R v_{\ell_k}(k_3) \frac{i}{(k_1+k_2)^2 - M_Y^2} \\ &\quad \times \bar{u}_{\ell_i}(k_1)(\mathcal{O}_{Yij} + \mathcal{O}_{Yji})P_L v_{\ell_j}(k_2),\end{aligned}\tag{13}$$

$$\begin{aligned}i\mathcal{M}_{s1} &= (-1)(-ig_s)^2 \bar{v}_{\ell_l}(p)(\mathcal{O}_{sli}P_L + \mathcal{O}_{sil}P_R)v_{\ell_i}(k_1) \frac{i}{(k_2+k_3)^2 - M_s^2} \\ &\quad \times \bar{u}_{\ell_k}(k_3)(\mathcal{O}_{skj}P_L + \mathcal{O}_{sjk}P_R)v_{\ell_j}(k_2),\end{aligned}\tag{14}$$

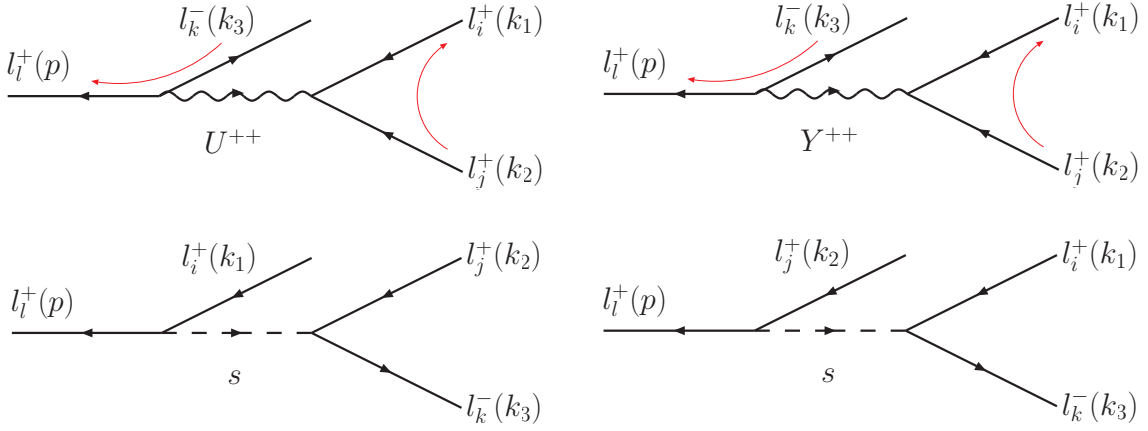


FIG. 1: Explicit diagrams contributing to the 3-body lepton decays.

TABLE II: Current experimental limits on every channel of 3-body lepton decay.

Process	BR
$\mu^+ \rightarrow e^+ e^- e^+$	$< 1.0 \times 10^{-12}$
$\tau^+ \rightarrow e^+ e^- e^+$	$< 2.7 \times 10^{-8}$
$\tau^+ \rightarrow e^+ \mu^- \mu^+$	$< 2.7 \times 10^{-8}$
$\tau^+ \rightarrow \mu^+ e^- e^+$	$< 1.8 \times 10^{-8}$
$\tau^+ \rightarrow \mu^+ \mu^- \mu^+$	$< 2.1 \times 10^{-8}$
$\tau^+ \rightarrow \mu^+ e^- \mu^+$	$< 1.7 \times 10^{-8}$
$\tau^+ \rightarrow e^+ \mu^- e^+$	$< 1.5 \times 10^{-8}$

$$i\mathcal{M}_{s2} = (-ig_s)^2 \bar{v}_{\ell_l}(p) (\mathcal{O}_{slj} P_L + \mathcal{O}_{sjl} P_R) v_{\ell_j}(k_2) \frac{i}{(k_1 + k_3)^2 - M_s^2} \times \bar{u}_{\ell_k}(k_3) (\mathcal{O}_{ski} P_L + \mathcal{O}_{sik} P_R) v_{\ell_i}(k_1). \quad (15)$$

A didactic discussion on how to achieve this expressions from the Lagrangians in Eq. (10) is presented on Appendix A. Nevertheless, we cross check the amplitudes above by generating them through **FeynRules** [30] in association with the **FeynArts** [31] package.

The current experimental limits on 3-body lepton decays are shown on Table II (see [32] and references therein). What we call *solutions* are any sets of numbers identified with the free parameters which cause the branching ratios to obey the constraints.

The range for the non-mass parameters are as follows

$$\begin{aligned} 0 &\leq \phi, \psi < 2\pi, \\ 0 &\leq \theta < \pi, \\ -1 &< \mathcal{O}_{Yij}, \mathcal{O}_{sij} < 1, \end{aligned} \quad (16)$$

which are chosen to exhaust the V_U space and keep the scalar interactions perturbative.

Moreover, because masses smaller than it are extremely unlikely and because the verification of this possibility wouldn't change the qualitative results of our analysis, we limit ourselves to masses above 500 GeV.

The solutions are obtained through a simple constrained global optimization routine, repeated for more than 100 random seeds to verify the stability of the best results.

IV. RESULTS AND ANALYSIS

In the scenarios where the $U^{\pm\pm}$ is present, we search for solutions which prioritize its mass – i.e., we seek sets of numbers which minimize M_U , with every other parameter, including M_s, M_Y , free. We make this choice because

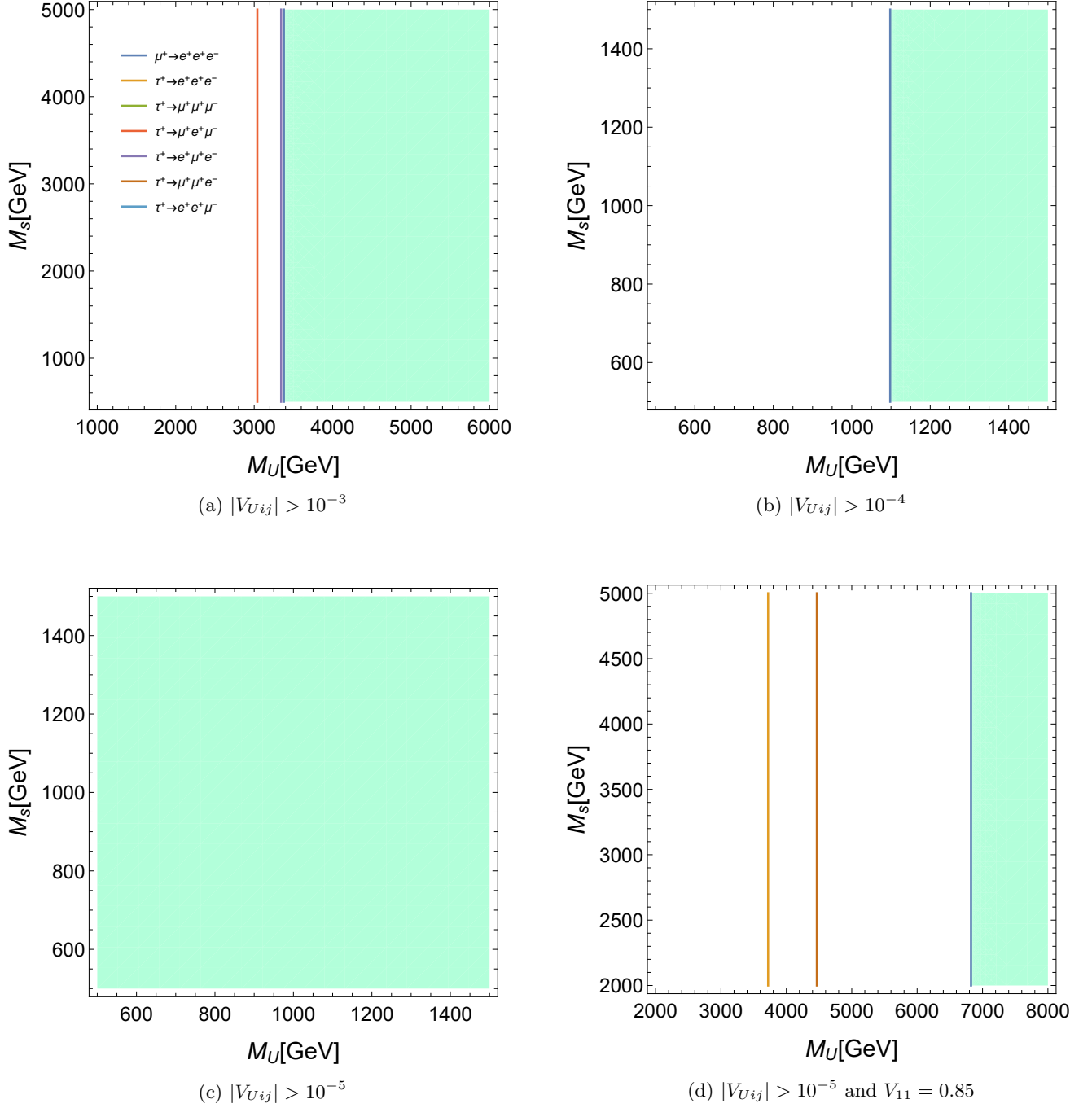


FIG. 2: Exclusion ranges for M_U generated by the experimental bounds on the various branching ratios for leptonic decays, for each of our 4 benchmark cases. The allowed region is painted green.

vector bosons usually and for a greater part of parameter space impose stronger constraints, but, specially, because the predicted unitarity of the bilepton mixing sets it apart phenomenologically and makes it a hardly constrained field. The achievement and examination of these solutions is the operational objective of this work.

Besides what has already been discussed, we consider additional benchmark conditions to fix the lower bound on the modulus of matrix elements – because of reasons exposed in the previous section. These conditions are detailed in the Figures and in the subsections below.

In addition, we consider benchmark impositions on the diagonal couplings of the mixing matrices. Also very restrictive, these constraints are designed to check what the lowest possible masses are if the model that correctly

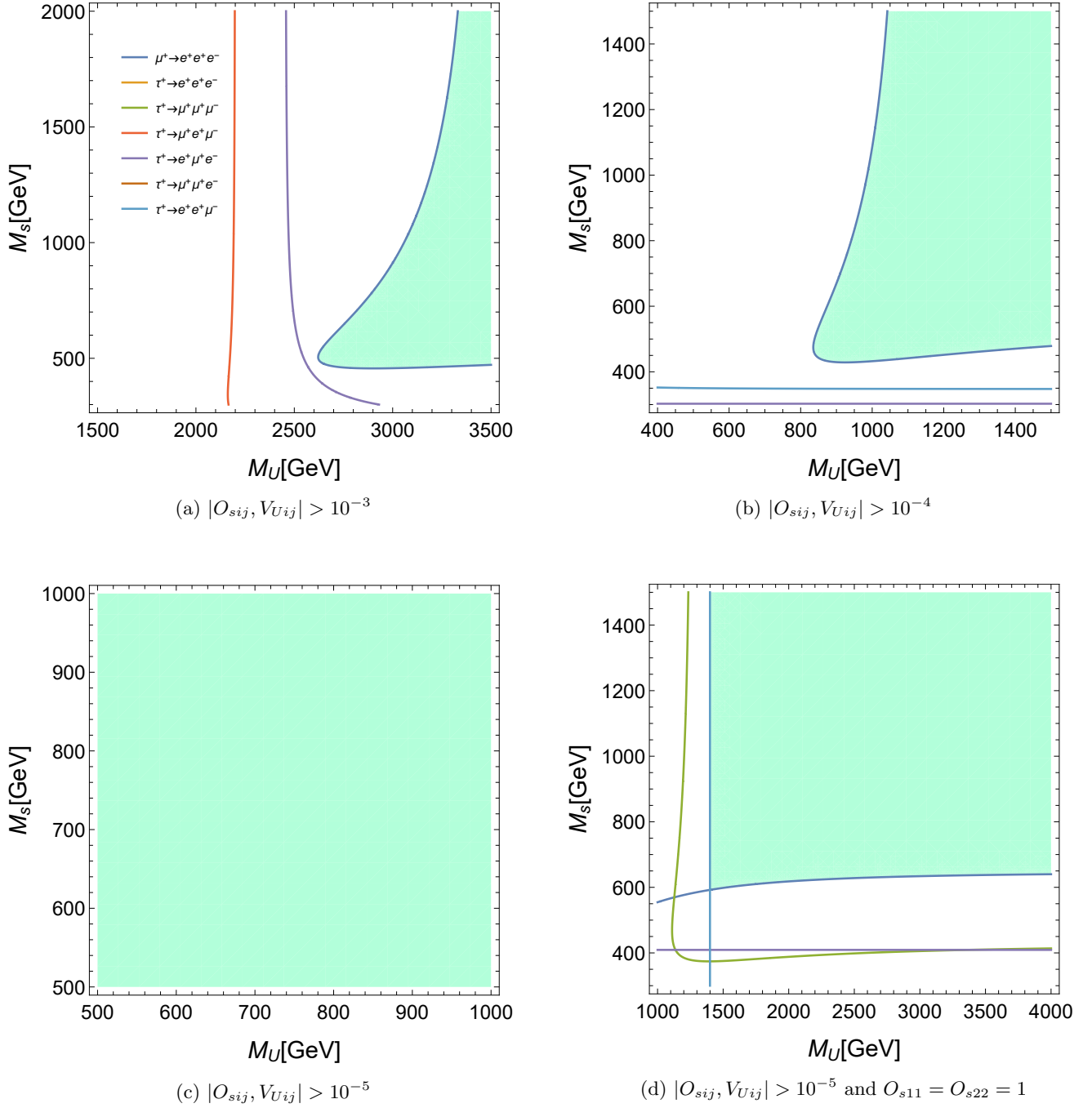


FIG. 3: Exclusion contours on the $M_U \times M_s$ plane generated by the bounds on 3-body Lepton Flavor Violating decays. The allowed region is painted green.

describes nature couples equal flavor particles (almost) maximally.

A. Pure U Scenario

We begin examining the constraints resulting from a doubly-charged vector bilepton alone. The results are presented in Figure 2 and the solutions in Table III. We show the contours in the $M_U \times M_s$ plane even though there is no M_s dependence to facilitate comparison with the scenario below.

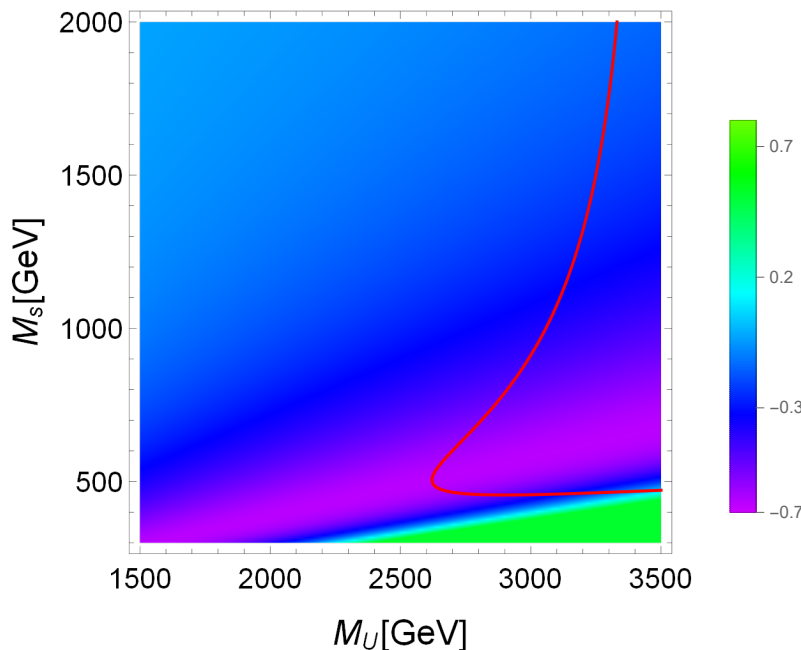


FIG. 4: Density plot of the extra contributions to $\mu^+ \rightarrow e^+ e^- e^+$, caused by the addition of the neutral scalar s to a model with the doubly-charged vector bilepton $U^{\pm\pm}$.

To allow for masses of the order of 1100 GeV (see Fig. 2b) we need an hierarchy¹ within V_U already similar to that of the Yukawa sector for quarks in the SM. But the greatest feature to observe is that with small general hierarchy (Fig. 2a) or with large diagonal coupling (Fig. 2d) the constraints are strong, demanding $M_U > 3200$ GeV and $M_U > 6900$ GeV, respectively. If there is no interference with extra particles capable of strongly altering this behaviour, this is enough to exclude often used benchmark points or substitute weaker exclusion ranges derived in the LHC phenomenology literature for this particle [22, 33–44], which is produced according to assumptions analogous to those contained in the mentioned cases.

It must be recognized that, in each instance, the contours result from a specific, not always evident, interplay between one or various BR bounds and the unitarity conditions of V_U .

B. $U - s$ Scenario

The scenario which includes a doubly-charged vector bilepton and a neutral scalar is the most complex and illuminating one, because it contains the unitary V_U matrix and possibly strong interference. The exclusion contours are shown in Figures 3 and the solutions appear at Table IV.

From the contours, we learn that to allow for bilepton masses of the order of $M_U < 1$ TeV, at least some effective couplings $g_{\text{eff}} \sim g_U V_{Uij}$ must be set as low as $< 10^{-4}$, meanwhile the entire parameter space is possible if the matrix elements are allowed to become as small as 10^{-5} . In particular, if the relevant coupling is numerically fixed through a benchmark that neglects mixing, like $g_{\text{eff}} \sim g_U = \frac{g_{2L}}{\sqrt{2}}$, which is generally done in the literature, then masses excessively larger than those searched and considered in the corresponding theoretical studies focused at the LHC are already excluded. Additionally, regarding the neutral scalar boson s , we observe, in Figure 3d, that if $\mathcal{O}_{s11} = \mathcal{O}_{s22} = 1$ is enforced, the bound on M_U is strengthened from² $M_U > 500$ GeV to $M_U > 1500$ GeV while virtually unchanging the bound on M_s . This just reasserts that the vector contribution is indeed dominant, which, again, could be expected from the unitarity of V_U and the fact that there is less possibilities in spin space for a scalar mediated process.

We also show, in Figure 4 a density plot of the ratio

$$\frac{\text{BR}_{U-s} + \text{BR}_s}{\text{BR}_U}, \quad (17)$$

¹ Since, a unitary matrix, small elements imply the need for large ones.

² We stress that 500 GeV is simply the lowest mass point we consider.

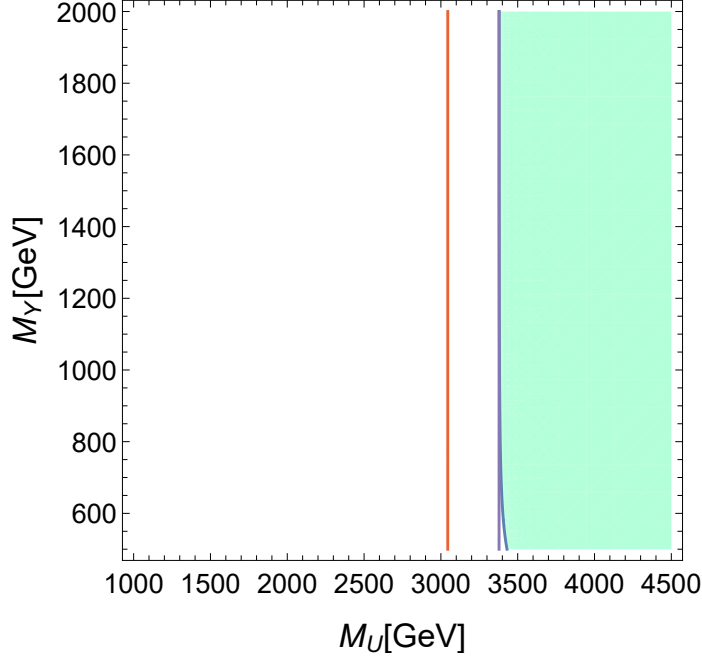


FIG. 5: Exclusion contour on the $M_U \times M_Y$ plane, showing that the solution subjected to the $|O_{Yij}, V_{Uij}| > 10^{-3}$ condition which gives the weakest bounds on the M_U mass is analogous to the one of the pure $U^{\pm\pm}$ case, with negligible scalar contributions (except when the mass of the scalar is exceedingly low, of course).

where BR_{X-Y} is the contribution of the interference between X and Y and BR_X is the pure X contribution to the BR. This information is useful to investigate how the presence of a second particle may relieve naive constraints derived from single exotic particle Lagrangians. We notice that, even if the scalar contribution is significantly smaller, it allows the solution to enhance destructive interference, which causes the distortion on the inferior left corner of the contour and contributes to, in the $|O_{sij}, V_{Uij}| > 10^{-3}$ case, rendering constraints softer by 19% on M_U .

C. $U - Y$ Scenario

This construction is simpler and the results can be inferred with reasoning alone.

The interference terms of the $U^{\pm\pm}$ with the $Y^{\pm\pm}$ -particle in the $\mu^+ \rightarrow e^+e^-e^+$ branching ratio are proportional to the electron mass, therefore interference effects are negligible to our purposes because m_e is much smaller than the next mass scale. This indicates that possible solutions for this scenario involve parameters, related to the vector bilepton, identical to those of the pure $U^{\pm\pm}$ scenario, of Section IV A, with $Y^{\pm\pm}$ -related parameters very small in modulus, the least allowed by the benchmark conditions. This guarantees that the $Y^{\pm\pm}$ contribution is rendered negligible and doesn't affect the exclusion contour, turned similar to those of Figure 2.

To illustrate the point above, we show, at Figure 5 the plot corresponding to the solution of Fig. 2a together with $O_{Yij} = 10^{-3}$.

D. $Y - s$ Scenario

The double scalar scenario is even less involved. The interference is, again, proportional to m_e , and there is no unitary mixing. Consequently, the structure of the solution is such that lower masses become allowed with diminishing couplings. We enforce that the scalar masses are nearly degenerate, with which we see, from Figure 6, that couplings of the order $g_{\text{eff}} \sim O_{sij} \sim 10^{-2}$ allow for scalar masses of the order of 2.5 TeV, while couplings as small as 10^{-3} are

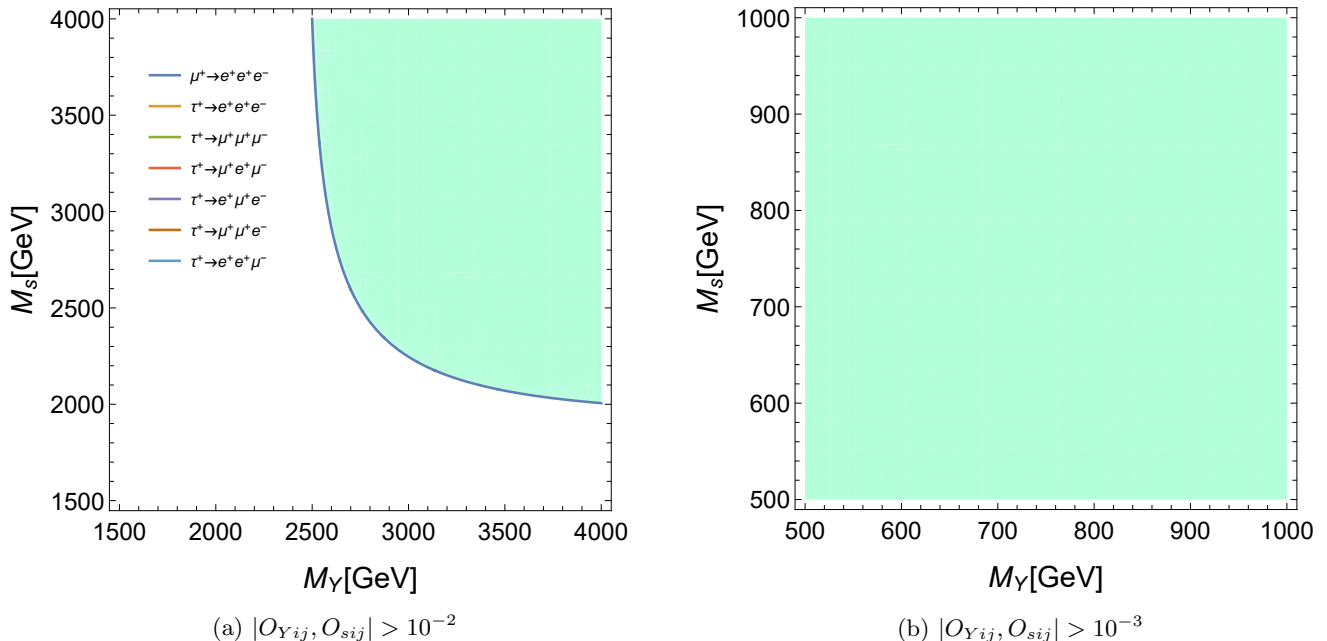


FIG. 6: Exclusion contours on the $M_Y \times M_s$ plane for bosons constrained to have similar masses.

permissive of low masses. It is easy to notice that, in this case, since there is neither conditions tying different matrix elements together nor interference, the strongest bound, *i.e.*, that of $\mu \rightarrow 3e$, is the only one that matters.

V. CONCLUSIONS

One important aspect in the search for new physics is knowing where to look, so that a common goal in BSM phenomenology is to impose constraints on exotic parameters, specially, lower bounds on masses. The high explorable energies and the excited stage of high amount of data collection reached by the LHC make it one ideal tool in this line of work.

Specifically, it has been used to derive constraints on M_U , the mass of a doubly charged vector bilepton, rare feature of BSM models. The collective result of these LHC efforts and also of other kinds of searches, such as precision muonium-antimuonium conversion [45], is well described by the bound $M_U \gtrsim 1$ TeV.

However, the bound above is derived through constructions that neglect the V_U mixing of the U - ll interaction [33–44] (an exception is the work in Ref. [22], which takes it into account through a very simplified construction). This unitary mixing matrix is predicted by a skeptical analysis and definition of the interaction form and, for a vector bilepton, cannot be ignored. We show, in a detailed way, that, once this mechanism is taken into account, the simple bounds on branching ratios of 3-body lepton decays produce model-independent constraints much stronger than the current theoretical bounds. To see this, it is enough to regard the pure $U^{\pm\pm}$ scenario, in which our study predicts $M_U > 3200$ GeV if the hierarchy within V_U is lesser than 10^{-3} and $M_U > 6900$ GeV with $|(V_U)_{ee}| = 0.85$. This last benchmark is illustrative of what is usually set in the literature, and our result is that the model-independent bounds from purely leptonic CLFV decays are much stronger than the naive constraints.

We don't primarily intend to achieve new specific mass bounds for the scalars: these particles interactions are not governed by unitary mixing, and there are concrete (model-dependent) experimental bounds for the doubly-charged scalar [46, 47], but, specially, the neutral scalar is a well known and common particle, analogous to the Higgs boson, so that its phenomenology is well understood in most models where it is present [48–51]. Nevertheless, we consider a pure scalar $Y - s$ scenario and what we find is that for low masses to be possible after enforcement of the CLFV bounds, the effective coupling must be of order of 10^{-3} . For comparison, the corresponding SM H - ee and H - $\tau\tau$ couplings are given by $(\mathcal{O})_e \sim 2.07 \times 10^{-6}$ and $(\mathcal{O})_\tau \sim 7.24 \times 10^{-3}$, indicating that it is certainly reasonable for an exotic flavor violating CP -even neutral scalar, generally associated with higher characteristic mass scales, to possess interactions parametrized by effective couplings of the order necessary for its mass to be possibly low.

The addition of the scalar bosons to our analysis is mainly intended to aid us understand the part that secondary,

non-dominant, particles can play altering the naive exclusion contours of dominant degrees of freedom, which, in the present context, occurs when it is considered together with the $U^{\pm\pm}$. We observe that the balance between the $U^{\pm\pm}$ and s contributions occurs in a manner that, in the optimal interference region, the lower bound on the mass of the $U^{\pm\pm}$ is relieved by 20%. Although it could be argued that such phenomenon can only happen in small, fine-tuned regions of parameter space, this behaviour can happen in a general multi-particle scenario, specially in ones where a subset of parameters are constrained by exterior phenomenological or theoretical input, such as the fitting of well measured distinct masses or mixing parameters, such as, for instance, a PMNS-like matrix which, in a given model, is dependent on the matrices lepton mixing matrices $V_{L,R}$.

ACKNOWLEDGEMENTS

MB would like to thank CNPq for the financial support and is specially grateful to Vicente Pleitez and Rodolfo Capdevilla for several useful discussions. JMD thanks to the Conacyt program Investigadoras e Investigadores por México, project 1753.

Appendix A: Deriving the amplitudes

To correctly derive amplitudes from Lagrangians with explicit charge conjugation can be troublesome. The issue appears because when these fields make up the interaction there is generally more than a way to contract a spinor chain with initial and final states, in which case simply writing the vertices with an explicit charge conjugation matrix is not by itself a well defined and unambiguous process. Below we show how to arrive at the amplitudes corresponding to the doubly-charged vector and scalar boson mediation, which suffer from this complication. We follow the algorithm and refer to the description of Refs. [52, 53], but focusing on the matter of dealing with Lagrangians with explicit charge conjugation, in the form as would naturally emerge from a renormalizable fundamental gauge theory.

We begin defining how to write down the spinor structure. Each spinor line in a diagram will come together with an Arbitrary Fermion Flow Arrow (AFFA) – recall that the true fermion flow is not continuous in this type of graph. With reference to this arbitrarily drawn line and the true fermion flow arrow, the rules for external fermion lines are

$$\begin{array}{cccc}
 \begin{array}{c} \xrightarrow{\text{red}} \\ \xrightarrow{k} \end{array} = u &
 \begin{array}{c} \xleftarrow{\text{red}} \\ \xrightarrow{k} \end{array} = \bar{v} &
 \begin{array}{c} \xrightarrow{\text{red}} \\ \xleftarrow{k} \end{array} = \bar{u} &
 \begin{array}{c} \xleftarrow{\text{red}} \\ \xleftarrow{k} \end{array} = v \\
 \begin{array}{c} \xleftarrow{\text{red}} \\ \xleftarrow{k} \end{array} = \bar{v} &
 \begin{array}{c} \xrightarrow{\text{red}} \\ \xleftarrow{k} \end{array} = u &
 \begin{array}{c} \xleftarrow{\text{red}} \\ \xrightarrow{k} \end{array} = v &
 \begin{array}{c} \xrightarrow{\text{red}} \\ \xrightarrow{k} \end{array} = \bar{u}
 \end{array}$$

Then we read the vertices off of the Lagrangians (5) and (7). Considering always incoming bosons, we have a first set of vertices, corresponding to the case in which the AFFA ends on the heaviest fermion, for each charge of the boson:

$$\begin{array}{c}
 \begin{array}{c} l_a^+ \\ \nearrow \\ U^{++} \\ \searrow \\ l_b^+ \end{array} \\
 = \Gamma_{ba}^{U^{++}} = \frac{g_{2L}}{\sqrt{2}} \gamma^\mu [P_L(V_U)_{ab} - P_R(V_U)_{ba}],
 \end{array} \tag{A1}$$

$$\begin{array}{c}
 \begin{array}{c} l_a^- \\ \nearrow \\ U^{--} \\ \searrow \\ l_b^- \end{array} \\
 = \Gamma_{ba}^{U^{--}} = \frac{g_{2L}}{\sqrt{2}} \gamma^\mu [P_L(V_U^\dagger)_{ab} - P_R(V_U^\dagger)_{ba}],
 \end{array} \tag{A2}$$

The formulas above are valid even when $a = b$, which can be seen symmetrizing the corresponding part of Lagrangian (5) as $\bar{\ell}_a^c \gamma^\mu P_L \ell_a = \frac{1}{2} [\bar{\ell}_a^c \gamma^\mu P_L \ell_a - \bar{\ell}_a^c \gamma^\mu P_R \ell_a]$.³ The remaining relative factor of 1/2 is compensated in the rule by a factor of 2 due to the identical particles. These vertices are called *regular*.

The seemingly innocuous choice of leaving the heaviest fermion on the right on the Lagrangians made in Section II is what amounts to defining the above vertices as the regular ones.

The second set of vertices for the $U^{\pm\pm}$ is obtained conjugating the original vertex by the charge conjugation matrix like $\Gamma' = C\Gamma C^{-1}$ – this recipe comes directly by transposition and manipulation of the reference spinor chain. We have that $C\gamma^\mu [P_L(V_U)_{ab} - P_R(V_U)_{ba}]C^{-1} = \gamma^\mu [P_L(V_U)_{ba} - P_R(V_U)_{ab}]$, so that the new vertex rule is $\Gamma'_{ab} = \Gamma_{ba}$. We write the reversed vertices for completeness (recall that ℓ_b is the heaviest of the 2 leptons)

A Feynman diagram showing a wavy line labeled U^{++} on the left, which splits into two outgoing fermion lines labeled l_a^+ and l_b^+ on the right. A red curved arrow indicates a charge conjugation operation between the two outgoing lines.

$$= \Gamma_{ab}^{U^{++}} = i \frac{g_{2L}}{\sqrt{2}} \gamma^\mu [P_L(V_U)_{ba} - P_R(V_U)_{ab}], \quad (\text{A3})$$

A Feynman diagram showing a wavy line labeled U^{--} on the left, which splits into two outgoing fermion lines labeled l_a^- and l_b^- on the right. A red curved arrow indicates a charge conjugation operation between the two outgoing lines.

$$= \Gamma_{ab}^{U^{--}} = i \frac{g_{2L}}{\sqrt{2}} \gamma^\mu [P_L(V_U^\dagger)_{ba} - P_R(V_U^\dagger)_{ab}]. \quad (\text{A4})$$

As an example up to this point, we write the rule corresponding to the two different choices of AFFA for the subdiagrams (and not vertices representations) below

A Feynman diagram showing a wavy line labeled U^{++} on the right, which splits into two outgoing fermion lines labeled μ^+ and e^- on the left. A red curved arrow indicates a charge conjugation operation between the two outgoing lines.

$$= \bar{v}_\mu \Gamma_{\mu e}^{U^{++}} u_e, \quad (\text{A5})$$

A Feynman diagram showing a wavy line labeled U^{++} on the right, which splits into two outgoing fermion lines labeled μ^+ and e^- on the left. A red curved arrow indicates a charge conjugation operation between the two outgoing lines.

$$= \bar{v}_e \Gamma_{e\mu}^{U^{++}} u_\mu. \quad (\text{A6})$$

The vertices for the doubly-charged scalar are shown below

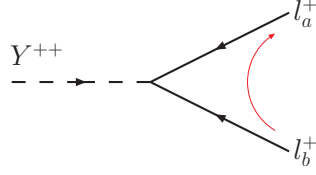
A Feynman diagram showing a dashed line labeled Y^{++} on the left, which splits into two outgoing fermion lines labeled l_a^+ and l_b^+ on the right. A red curved arrow indicates a charge conjugation operation between the two outgoing lines.

$$= \Gamma_{ba}^{Y^{++}} = -ig_{YL} [(\mathcal{O}_Y)_{ab} + (\mathcal{O}_Y)_{ba}] P_L, \quad (\text{A7})$$

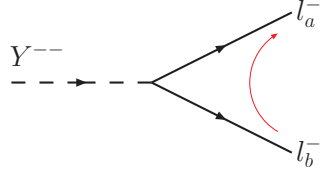
A Feynman diagram showing a dashed line labeled Y^{--} on the left, which splits into two outgoing fermion lines labeled l_a^- and l_b^- on the right. A red curved arrow indicates a charge conjugation operation between the two outgoing lines.

$$= \Gamma_{ba}^{Y^{--}} = -ig_{YL} [(\mathcal{O}_Y^\dagger)_{ab} + (\mathcal{O}_Y^\dagger)_{ba}] P_R, \quad (\text{A8})$$

³ Notice again that the vector part of this interaction dies out.



$$= \Gamma_{ab}^{Y^{++}} = -ig_{YL} [(\mathcal{O}_Y)_{ba} + (\mathcal{O}_Y)_{ab}] P_L, \quad (\text{A9})$$



$$= \Gamma_{ab}^{Y^{--}} = -ig_{YL} [(\mathcal{O}_Y^\dagger)_{ba} + (\mathcal{O}_Y^\dagger)_{ab}] P_R. \quad (\text{A10})$$

We emphasize one last time that what defines if a vertex is regular or reversed is the direction of the AFFA with respect to fermion generation – which, in turn, is a consequence of the conventional form of the Lagrangian.

Knowing the vertices and how to write the exotic spinor chains, the missing ingredient is the ability to find the relative sign between diagrams. This is the greatest reason for the necessity of an algorithm that substitutes the mere explicit use of the charge conjugation matrix. Within the algorithm, to find the relative signs amounts to simply comparing particle "order" – more precisely, the order in which spinors appear in the chain – with respect to the AFFA and identifying the order of the relating permutation.

Refer to our real diagrams of Fig. 1. The particle orders are (we label different particles by the momenta)

$$\begin{aligned} R(\mathcal{M}_U) &= (p, k_3, k_1, k_2), \\ R(\mathcal{M}_Y) &= (p, k_3, k_1, k_2), \\ R(\mathcal{M}_{s1}) &= (p, k_1, k_3, k_2), \\ R(\mathcal{M}_{s2}) &= (p, k_2, k_3, k_1). \end{aligned} \quad (\text{A11})$$

Taking $R(\mathcal{M}_U)$ as the referential, we identify that the only ordered set related to it by an odd permutation is $R(\mathcal{M}_{s1})$, so that $i\mathcal{M}_{s1}$ comes attached to an extra minus sign.

This concludes a sufficient description of how our amplitudes can be obtained from the given Lagrangians.

Appendix B: Solutions

TABLE III: Solutions of the pure U scenario, corresponding to the plots of Fig. 2.

Pure U : $ V_{Uij} > 10^{-3}$			
M_U	3380	ψ	1.48108
ϕ	3.03983	θ	2.66989
Pure U : $ V_{Uij} > 10^{-4}$			
M_U	1100	ψ	0.78535
ϕ	5.49774	θ	0.00014
Pure U : $ V_{Uij} > 10^{-5}$			
M_U	500	ψ	0.72066
ϕ	0.72067	θ	3.13801
Pure U : $ V_{Uij} > 10^{-5}$, $V_{U11} = 0.85$			
M_U	6830	ψ	4.74012
ϕ	4.68301	θ	0.55504

TABLE IV: Solutions of the $U - s$ scenario, respective of the plots shown in Fig. 3

$U - s: V_{Uij}, \mathcal{O}_{sij} > 10^{-3}$					
M_U	2650	\mathcal{O}_{s11}	3.11564×10^{-3}	\mathcal{O}_{s22}	1.43763×10^{-3}
M_s	500	\mathcal{O}_{s12}	3.01898×10^{-3}	\mathcal{O}_{s23}	4.06257×10^{-2}
ϕ	6.26303	\mathcal{O}_{s13}	4.20596×10^{-2}	\mathcal{O}_{s31}	-1.32129×10^{-1}
ψ	1.55218	\mathcal{O}_{s21}	3.19852×10^{-3}	\mathcal{O}_{s32}	1.51094×10^{-1}
θ	2.90919				
$U - s: V_{Uij}, \mathcal{O}_{sij} > 10^{-4}$					
M_U	840	\mathcal{O}_{s11}	2.57667×10^{-3}	\mathcal{O}_{s22}	-2.14209×10^{-3}
M_s	500	\mathcal{O}_{s12}	-3.29400×10^{-3}	\mathcal{O}_{s23}	-6.05650×10^{-2}
ϕ	1.45901	\mathcal{O}_{s13}	4.05147×10^{-1}	\mathcal{O}_{s31}	-4.81308×10^{-2}
ψ	1.45911	\mathcal{O}_{s21}	-3.34363×10^{-3}	\mathcal{O}_{s32}	-1.44602×10^{-1}
θ	3.13998				
$U - s: V_{Uij}, \mathcal{O}_{sij} > 10^{-5}$					
M_U	< 500	\mathcal{O}_{s11}	1.00000×10^{-5}	\mathcal{O}_{s22}	1.00000×10^{-5}
M_s	< 500	\mathcal{O}_{s12}	1.00000×10^{-5}	\mathcal{O}_{s23}	1.00000×10^{-5}
ϕ	0.72067	\mathcal{O}_{s13}	1.00000×10^{-5}	\mathcal{O}_{s31}	1.00000×10^{-5}
ψ	0.72066	\mathcal{O}_{s21}	1.00000×10^{-5}	\mathcal{O}_{s32}	1.00000×10^{-5}
θ	3.13801				
$U - s: V_{Uij}, \mathcal{O}_{sij} > 10^{-5}, \mathcal{O}_{s11} = \mathcal{O}_{s22} = 1$					
M_U	1800	\mathcal{O}_{s11}	1.00000	\mathcal{O}_{s22}	1.00000
M_s	580	\mathcal{O}_{s12}	-1.12685×10^{-5}	\mathcal{O}_{s23}	-8.60549×10^{-4}
ϕ	0.00020	\mathcal{O}_{s13}	-1.19611×10^{-3}	\mathcal{O}_{s31}	1.83141×10^{-4}
ψ	0.00024	\mathcal{O}_{s21}	-1.13022×10^{-5}	\mathcal{O}_{s32}	2.55491×10^{-3}
θ	3.09077				

-
- [1] S. T. Petcov, “The Processes $\mu \rightarrow e\gamma$, $\mu \rightarrow ee\bar{e}$, $\nu' \rightarrow \nu\gamma$ in the Weinberg-Salam Model with Neutrino Mixing,” *Sov. J. Nucl. Phys.* **25**, 340 (1977) [*Yad. Fiz.* **25**, 641 (1977)] Erratum: [*Sov. J. Nucl. Phys.* **25**, 698 (1977)] Erratum: [*Yad. Fiz.* **25**, 1336 (1977)].
 - [2] A. de Gouvea and P. Vogel, “Lepton flavor and Number Conservation, and Physics Beyond the Standard Model,” *Prog. Part. Nucl. Phys.* **71**, 75-92 (2013) doi:10.1016/j.pnpnp.2013.03.006 [arXiv:1303.4097 [hep-ph]].
 - [3] J. Heeck, “Interpretation of Lepton flavor Violation,” *Phys. Rev. D* **95**, no.1, 015022 (2017) doi:10.1103/PhysRevD.95.015022 [arXiv:1610.07623 [hep-ph]].
 - [4] G. Hernández-Tomé, G. López Castro and P. Roig, “flavor violating leptonic decays of τ and μ leptons in the Standard Model with massive neutrinos,” *Eur. Phys. J. C* **79**, no.1, 84 (2019) [erratum: *Eur. Phys. J. C* **80**, no.5, 438 (2020)] doi:10.1140/epjc/s10052-019-6563-4 [arXiv:1807.06050 [hep-ph]].
 - [5] R. H. Bernstein and P. S. Cooper, “Charged Lepton flavor Violation: An Experimenter’s Guide,” *Phys. Rept.* **532**, 27-64 (2013) doi:10.1016/j.physrep.2013.07.002 [arXiv:1307.5787 [hep-ex]].
 - [6] T. Mori and W. Ootani, “flavor violating muon decays,” *Prog. Part. Nucl. Phys.* **79**, 57-94 (2014) doi:10.1016/j.pnpnp.2014.09.001
 - [7] L. Calibbi and G. Signorelli, “Charged Lepton flavor Violation: An Experimental and Theoretical Introduction,” *Riv. Nuovo Cim.* **41**, no.2, 71-174 (2018) doi:10.1393/ncr/i2018-10144-0 [arXiv:1709.00294 [hep-ph]].
 - [8] A. M. Baldini *et al.* [MEG II], “The design of the MEG II experiment,” *Eur. Phys. J. C* **78**, no.5, 380 (2018) doi:10.1140/epjc/s10052-018-5845-6 [arXiv:1801.04688 [physics.ins-det]].
 - [9] T. Kraetzschmar [Belle-II], “First Results and Prospects for τ Lepton Physics at Belle II,” *PoS CHARM2020*, 042 (2021) doi:10.22323/1.385.0042 [arXiv:2111.13385 [hep-ex]].
 - [10] L. Guzzi [CMS], “Search for the $\tau \rightarrow \mu\mu\mu$ decay at CMS,” *Nuovo Cim. C* **43**, no.2-3, 47 (2020) doi:10.1393/ncc/i2020-20047-x
 - [11] K. Hayasaka, K. Inami, Y. Miyazaki, K. Arinstein, V. Aulchenko, T. Aushev, A. M. Bakich, A. Bay, K. Belous and V. Bhardwaj, *et al.* “Search for Lepton flavor Violating Tau Decays into Three Leptons with 719 Million Produced Tau+Tau- Pairs,” *Phys. Lett. B* **687**, 139-143 (2010) doi:10.1016/j.physletb.2010.03.037 [arXiv:1001.3221 [hep-ex]].
 - [12] J. C. Romao, A. Barroso, M. C. Bento and G. C. Branco, “Flavor Violation in Supersymmetric Theories,” *Nucl. Phys. B* **250**, 295-311 (1985) doi:10.1016/0550-3213(85)90483-3
 - [13] F. Borzumati and A. Masiero, “Large Muon and electron Number Violations in Supergravity Theories,” *Phys. Rev. Lett.* **57**, 961 (1986) doi:10.1103/PhysRevLett.57.961
 - [14] S. P. Martin, “A Supersymmetry primer,” *Adv. Ser. Direct. High Energy Phys.* **18**, 1-98 (1998) doi:10.1142/9789812839657_0001 [arXiv:hep-ph/9709356 [hep-ph]].
 - [15] W. Altmannshofer, A. J. Buras, S. Gori, P. Paradisi and D. M. Straub, “Anatomy and Phenomenology of FCNC and CPV Effects in SUSY Theories,” *Nucl. Phys. B* **830**, 17-94 (2010) doi:10.1016/j.nuclphysb.2009.12.019 [arXiv:0909.1333 [hep-ph]].
 - [16] S. Davidson and G. J. Grenier, “Lepton flavor violating Higgs and tau to mu gamma,” *Phys. Rev. D* **81**, 095016 (2010) doi:10.1103/PhysRevD.81.095016 [arXiv:1001.0434 [hep-ph]].
 - [17] A. Dery, A. Efrati, G. Hiller, Y. Hochberg and Y. Nir, “Higgs couplings to fermions: 2HDM with MFV,” *JHEP* **08**, 006 (2013) doi:10.1007/JHEP08(2013)006 [arXiv:1304.6727 [hep-ph]].
 - [18] J. Kopp and M. Nardecchia, “Flavor and CP violation in Higgs decays,” *JHEP* **10**, 156 (2014) doi:10.1007/JHEP10(2014)156 [arXiv:1406.5303 [hep-ph]].
 - [19] J. T. Liu and D. Ng, “Lepton flavor changing processes and CP violation in the 331 model,” *Phys. Rev. D* **50**, 548-557 (1994) doi:10.1103/PhysRevD.50.548 [arXiv:hep-ph/9401228 [hep-ph]].
 - [20] A. C. B. Machado, J. Montaña and V. Pleitez, “Lepton flavor violating processes in the minimal 3-3-1 model with sterile neutrinos,” *J. Phys. G* **46**, no.11, 115005 (2019) doi:10.1088/1361-6471/ab2bac [arXiv:1604.08539 [hep-ph]].
 - [21] J. M. Cabarcas, J. Duarte and J. A. Rodriguez, “Lepton Flavor Violation processes in 331 Models,” *PoS HQL2012*, 072 (2012) doi:10.22323/1.166.0072
 - [22] M. W. Barela and V. Pleitez, “Trimuon production at the LHC,” *Phys. Rev. D* **101**, no.1, 015024 (2020) doi:10.1103/PhysRevD.101.015024
 - [23] F. Pisano and V. Pleitez, “An $SU(3) \times U(1)$ model for electroweak interactions,” *Phys. Rev. D* **46**, 410-417 (1992) doi:10.1103/PhysRevD.46.410 [arXiv:hep-ph/9206242 [hep-ph]].
 - [24] P. H. Frampton, “Chiral dilepton model and the flavor question,” *Phys. Rev. Lett.* **69**, 2889 (1992). doi:10.1103/PhysRevLett.69.2889
 - [25] A. G. Dias, J. C. Montero and V. Pleitez, “Closing the $SU(3)(L) \times U(1)(X)$ symmetry at electroweak scale,” *Phys. Rev. D* **73**, 113004 (2006) doi:10.1103/PhysRevD.73.113004 [arXiv:hep-ph/0605051 [hep-ph]].
 - [26] P. H. Frampton and B. H. Lee, “ $SU(15)$ GRAND UNIFICATION,” *Phys. Rev. Lett.* **64**, 619 (1990) doi:10.1103/PhysRevLett.64.619
 - [27] P. H. Frampton and T. W. Kephart, “Higgs sector and proton decay in $SU(15)$ grand unification,” *Phys. Rev. D* **42**, 3892-3894 (1990) doi:10.1103/PhysRevD.42.3892
 - [28] M. W. Barela, “Can scalars matter? A vector bilepton phenomenologic example,” [arXiv:2112.01564 [hep-ph]].
 - [29] H. Georgi and S. Weinberg, “Neutral Currents in Expanded Gauge Theories,” *Phys. Rev. D* **17**, 275 (1978) doi:10.1103/PhysRevD.17.275

- [30] A. Alloul, N. D. Christensen, C. Degrande, C. Duhr and B. Fuks, “FeynRules 2.0 - A complete toolbox for tree-level phenomenology,” *Comput. Phys. Commun.* **185**, 2250-2300 (2014) doi:10.1016/j.cpc.2014.04.012 [arXiv:1310.1921 [hep-ph]].
- [31] T. Hahn, “Generating Feynman diagrams and amplitudes with FeynArts 3,” *Comput. Phys. Commun.* **140**, 418-431 (2001) doi:10.1016/S0010-4655(01)00290-9 [arXiv:hep-ph/0012260 [hep-ph]].
- [32] P. A. Zyla *et al.* [Particle Data Group], “Review of Particle Physics,” *PTEP* **2020**, no.8, 083C01 (2020) doi:10.1093/ptep/ptaa104
- [33] B. Dutta and S. Nandi, “Search for dilepton gauge bosons in hadron colliders,” *Phys. Lett. B* **340**, 86 (1994). doi:10.1016/0370-2693(94)91302-1
- [34] B. Dion, T. Gregoire, D. London, L. Marleau and H. Nadeau, “Bilepton production at hadron colliders,” *Phys. Rev. D* **59**, 075006 (1999) doi:10.1103/PhysRevD.59.075006 [hep-ph/9810534].
- [35] E. Ramirez Barreto, Y. A. Coutinho and J. S. Borges, “Vector-bilepton Contribution to Four Lepton Production at the LHC,” *Phys. Rev. D* **88**, 035016 (2013) doi:10.1103/PhysRevD.88.035016 [arXiv:1307.4683 [hep-ph]].
- [36] E. Ramirez Barreto, Y. A. Coutinho and J. Sa Borges, “Vector- and Scalar-Bilepton Pair Production in Hadron Colliders,” *Phys. Rev. D* **83**, 075001 (2011) doi:10.1103/PhysRevD.83.075001 [arXiv:1103.1267 [hep-ph]].
- [37] E. Ramirez Barreto, Y. A. Coutinho and J. Sa Borges, “Charged Bilepton Pair Production at LHC Including Exotic Quark Contribution,” *Nucl. Phys. B* **810**, 210-225 (2009) doi:10.1016/j.nuclphysb.2008.11.015 [arXiv:0811.0846 [hep-ph]].
- [38] A. Nepomuceno, B. Meirose and F. Eccard, “First results on bilepton production based on LHC collision data and predictions for run II,” *Phys. Rev. D* **94**, no. 5, 055020 (2016) doi:10.1103/PhysRevD.94.055020 [arXiv:1604.07471 [hep-ph]].
- [39] M. B. Tully and G. C. Joshi, “Mass bounds for flavor mixing bileptons,” *Phys. Lett. B* **466**, 333 (1999) doi:10.1016/S0370-2693(99)01161-2 [hep-ph/9905552].
- [40] B. Meirose and A. A. Nepomuceno, “Searching for doubly-charged vector bileptons in the Golden Channel at the LHC,” *Phys. Rev. D* **84**, 055002 (2011) doi:10.1103/PhysRevD.84.055002 [arXiv:1105.6299 [hep-ph]].
- [41] G. Corcella, C. Corianò, A. Costantini and P. H. Frampton, “Exploring Scalar and Vector Bileptons at the LHC in a 331 Model,” *Phys. Lett. B* **785**, 73-83 (2018) doi:10.1016/j.physletb.2018.08.015 [arXiv:1806.04536 [hep-ph]].
- [42] G. Corcella, C. Coriano, A. Costantini and P. H. Frampton, “Bilepton Signatures at the LHC,” *Phys. Lett. B* **773**, 544-552 (2017) doi:10.1016/j.physletb.2017.09.015 [arXiv:1707.01381 [hep-ph]].
- [43] C. Corianò and P. H. Frampton, “Possible Bilepton Resonances in Like-Sign Pairs,” *Mod. Phys. Lett. A* **34**, no.10, 1950076 (2019) doi:10.1142/S0217732319500767 [arXiv:1812.02723 [hep-ph]].
- [44] P. H. Frampton, “Using LHC to Discover the Bilepton,” *PoS CORFU2019*, 098 (2020) doi:10.22323/1.376.0098
- [45] A. Gusso, C. A. de S. Pires and P. S. Rodrigues da Silva, *J. Phys. G* **30**, 37-44 (2004) doi:10.1088/0954-3899/30/2/004 [arXiv:hep-ph/0208062 [hep-ph]].
- [46] M. Aaboud *et al.* [ATLAS], “Search for doubly charged Higgs boson production in multi-lepton final states with the ATLAS detector using proton–proton collisions at $\sqrt{s} = 13$ TeV,” *Eur. Phys. J. C* **78**, no.3, 199 (2018) doi:10.1140/epjc/s10052-018-5661-z [arXiv:1710.09748 [hep-ex]].
- [47] G. Aad *et al.* [ATLAS], “Search for anomalous production of prompt same-sign lepton pairs and pair-produced doubly charged Higgs bosons with $\sqrt{s} = 8$ TeV pp collisions using the ATLAS detector,” *JHEP* **03**, 041 (2015) doi:10.1007/JHEP03(2015)041 [arXiv:1412.0237 [hep-ex]].
- [48] M. Aaboud *et al.* [ATLAS], “Search for additional heavy neutral Higgs and gauge bosons in the ditau final state produced in 36 fb^{-1} of pp collisions at $\sqrt{s} = 13$ TeV with the ATLAS detector,” *JHEP* **01**, 055 (2018) doi:10.1007/JHEP01(2018)055 [arXiv:1709.07242 [hep-ex]].
- [49] A. M. Sirunyan *et al.* [CMS], “Search for additional neutral MSSM Higgs bosons in the $\tau\tau$ final state in proton-proton collisions at $\sqrt{s} = 13$ TeV,” *JHEP* **09**, 007 (2018) doi:10.1007/JHEP09(2018)007 [arXiv:1803.06553 [hep-ex]].
- [50] G. Aad *et al.* [ATLAS], “Combined measurements of Higgs boson production and decay using up to 80 fb^{-1} of proton-proton collision data at $\sqrt{s} = 13$ TeV collected with the ATLAS experiment,” *Phys. Rev. D* **101**, no.1, 012002 (2020) doi:10.1103/PhysRevD.101.012002 [arXiv:1909.02845 [hep-ex]].
- [51] M. Aaboud *et al.* [ATLAS], “Search for invisible Higgs boson decays in vector boson fusion at $\sqrt{s} = 13$ TeV with the ATLAS detector,” *Phys. Lett. B* **793**, 499-519 (2019) doi:10.1016/j.physletb.2019.04.024 [arXiv:1809.06682 [hep-ex]].
- [52] A. Denner, H. Eck, O. Hahn and J. Kublbeck, *Feynman rules for fermion number violating interactions*, *Nucl. Phys. B* **387**, 467 (1992).
- [53] A. Denner, H. Eck, O. Hahn and J. Kublbeck, *Compact Feynman rules for Majorana fermions*, *Phys. Lett. B* **291**, 278 (1992).